Jugović, D., M. Mitrić, M. Kuzmanović, N. Cvjetićanin, S. Marković, S. Škapin, and D. Uskoković. "Rapid Crystallization of LiFePO4 Particles by Facile Emulsion-Mediated Solvothermal Synthesis." *Powder Technology* 219 (March 2012): 128–34. http://dx.doi.org/10.1016/j.powtec.2011.12.028

Rapid crystallization of $LiFePO_4$ particles by facile emulsion-mediated solvothermal synthesis

D. Jugović [a], M. Mitrić [b], M. Kuzmanović [a], N. Cvjetićanin [c], S. Marković [a], S. Škapin [d], and D. Uskoković [a]

[a]Institute of Technical Sciences of SASA, Knez Mihailova 35/IV, 11 000 Belgrade, Serbia

[b]The Vinča Institute of Nuclear Sciences, University of Belgrade, P.O. Box 522, 11 001 Belgrade, Serbia

[c]Faculty of Physical Chemistry, University of Belgrade, Studentski trg 12-16, P.O. Box 137, Belgrade, Serbia

[d]Jožef Štefan Institute, Jamova 39, SI-1000 Ljubljana, Slovenia

Abstract

Lithium iron phosphate powders were obtained by solvothermal treatments of quaternary emulsions Triton X-100/cyclohexane/*n*-hexanol/water at low temperature (180 ºC), with or without stirring. Such synthesis conditions allowed for fast crystallization of pure olivine-type $LiFePO_4$ powder, evidenced by the X-ray powder diffraction measurements and energy dispersive spectroscopy. It has been found that stirring drastically changes the morphology of $LiFePO_4$ particles, causing a preferential crystal orientation. Also, a great difference in the morphology was demonstrated by field emission scanning electron microscopy. The powder obtained after only half an hour of the dynamic solvothermal treatment, without additional post annealing, and without carbon coating, was electrochemically active, showing the discharge capacity of 115 mAh/g.

Keywords: Lithium iron phosphate ($LiFePO_4$); electrode materials; X-ray diffraction; scanning electron microscopy

Corresponding author: Dr. Dragana Jugović

Phone: +381641177549, Fax: +381112185263,
e-mail: dragana.jugovic@itn.sanu.ac.rs; djugovic@vinca.rs

1. Introduction

Lithium iron phosphate ($LiFePO_4$) is widely considered a promising cathode material for high-rate Li-ion rechargeable batteries. The benefits of using $LiFePO_4$ are the following: excellent cycle life, high structural stability, low cost and environmental friendliness. Lithium iron phosphate can utilize one lithium ion per formula unit, which leads to the theoretical capacity of 170 $mAhg^{-1}$. The main obstacles in reaching the theoretical capacity are its low electronic and low ionic conductivity. These transport limitations can be overcome by decreasing the particle size [1-3] and/or by coating the particles with some conductive material such as carbon, the most frequently used material [4-9].

The olivine structure that typifies $LiFePO_4$ has a slightly distorted hexagonal close-packed oxygen array (in space group no. 62 Pnma), Figure 1. Divalent Fe^{2+} ions occupy corner-shared octahedra (denoted as M2 sites). The phosphorus ions are located in tetrahedral sites, and the lithium ions reside in chains of edge-shared octahedra (M1 sites) [10, 11]. Within such a crystal structure, lithium motion is confined to one-dimensional (1D) channels along the b axis [12].

Beginning with the discovery of the electrochemical properties of the olivine phase by Padhi et al. in 1997 [10], numerous ways of synthesis of the olivine-type $LiFePO_4$ have been explored [13]. Many of these synthetic routes are both time- and energy-consuming. Driven by the energy crisis, researchers presently favor low-temperature synthesis methods, such as hydrothermal processing [3, 14, 15], and explore novel synthesis approaches, such as ionothermal synthesis [16, 17]. Solvothermal processing is a low-temperature effective method to prepare materials with well-defined morphology, scarcely used in the synthesis of $LiFePO_4$ particles. So far, several solvents were used for the synthesis of $LiFePO_4$ powders of different morphologies, such as ethylene glycol [18, 19, 20], PEG [21], benzyl alcohol [22], and ethanol [14]. However, in most cases, the obtained materials had a low crystallization degree, and post-heat treatments were required to achieve sufficiently crystalline particles; therefore, many authors argue that

the $LiFePO_4$ obtained using this method is not made at low temperatures. A proper surfactant in solvothermal systems can tune the particle size and morphology owing to the adsorption of surfactant molecules onto the particle surface during particle growth. A poly(vinyl pyrrolidone) (PVP) [22], hexadecyltrimethylammonium bromide (CTAB) [23], oleic acid [18], etc. were used as surfactants in the synthesis of $LiFePO_4$. However, to our best knowledge the use of a surfactant commercially known as Triton X-100 in the synthesis of $LiFePO_4$ powders has not been explored yet. Xua et al. reported the microemulsion synthesis of $LiFePO_4$ particles, which was actually a nucleation step prior to high temperature treatment [23]. In the present study, we combined reverse micelles and the solvothermal route in order to achieve one-pot synthesis of $LiFePO_4$ particles at a low temperature (180 ºC) without an additional high-temperature treatment. The quaternary emulsions of Triton X-100/cyclohexane/*n*-hexanol/water were solvothermally treated for various time periods with and without stirring. Such synthesis conditions allowed for a fast crystallization of pure olivine-type $LiFePO_4$ powder. In addition, stirring drastically changes the morphology of $LiFePO_4$ particles causing a preferential crystal orientation.

2. Experimental

2.1. Synthesis of $LiFePO_4$ powders

The powders of $LiFePO_4$ were prepared by a solvothermal treatment of quaternary emulsions Triton X-100/cyclohexane/*n*-hexanol/water. Our intention was to produce a morphology similar to the $LaVO_4$ nanowires obtained by Fan et al. [24]; therefore, we used similar procedure, except for the surfactant. In a typical synthesis, Triton X-100 was used as the surfactant, cyclohexane was used as the oil phase, and *n*-hexanol was used as a cosurfactant. They were mixed in the following volumes: 3, 20, and 2.5 ml, respectively. The resulting solution was divided into two parts in order to obtain two emulsions, namely, emulsion A and emulsion B. Emulsion A was obtained by adding 7 ml of 2.5 M LiOH aqueous solution to the above solution. Then the equimolar (0.006 mol) amounts of $FeSO_4*7H_2O$, $(NH_4)_2HPO_4$, and citric acid were dissolved in 8 ml of

water and added to another part of the solution, i.e. emulsion B. Citric acid is here used as a reductant to prevent the Fe^{2+} oxidation. The emulsion that was further solvothermally treated was obtained by adding emulsion A to emulsion B under substantial stirring, with the Li:Fe:P ratio of 3:1:1. Precipitation occured immediately after these two emulsions had been mixed. Prior to the solvothermal treatment, the emulsion was simmered with argon to release oxygen, and sealed in a 60 ml Teflon-lined stainless steel autoclave. The sealed autoclave was then immersed into a silicon oil bath, previously heated at 180 °C, on the magnetic stirrer hotplate (Figure 2). The solvothermal treatments were performed for various time periods: 0.5, 1, 3, 15, and 100 hours, with or without constant stirring. The obtained powders were centrifuged, washed several times with ethanol and water, and dried.

2.2. Material characterization

The X-ray powder diffraction data were collected on a Philips PW 1050 diffractometer with Cu-K$\alpha_{1,2}$ radiation (Ni filter) at room temperature. Measurements were done over the 2θ range of 15-70° with a scanning step width of 0.05° and 3-s time per step for each sample.

The morphology of the synthesized powders was analyzed by field emission scanning electron microscopy (FE-SEM, Supra 35 VP, Carl Zeiss).

The particle size distributions were determined by a particle size analyzer (PSA) Mastersizer 2000 (Malvern Instruments Ltd., UK). For the purpose of particle size measurements, the powder was dry deagglomerated in an ultrasonic bath (frequency of 40 kHz and power of 50 W) for 60 min.

2.3. Electrochemical testing

The electrochemical measurements were carried out in a closed, argon-filled two-electrode cell, with a metallic lithium counter electrode. 1M solution of $LiClO_4$ (p.a., Chemetall GmbH) in PC (p.a., Honeywell) was used as an electrolyte. Working electrodes were made from as-prepared materials, carbon black and polyvinylidene

fluoride (PVdF, Aldrich) mixed in a 75:20:5 weight percent ratio and deposited on platinum foils from a slurry prepared in N-methyl-2-pyrrolidone. The galvanostatic charge/discharge tests were performed between 4.2 and 2.3 V at C/10 current rates.

3. Results and Discussion

3.1. Morphology studies

The particle morphology of the samples was revealed by field emission scanning electron microscopy (FESEM). The images of the powders, obtained during the solvothermal treatment at 180 ºC for various time periods with and without stirring, are presented in Figures 3-8. Interestingly, after only half an hour of the treatment, different morphologies of the powders could be observed depending on the mode of the solvothermal treatment – dynamic or static. Namely, the powder prepared in the static mode, without stirring, consists of small irregular strongly agglomerated particles (Figure 3), with spheroid-like agglomerates that vary in size from 0.15 to 1.15 μm. These agglomerates of nodular structure have rough surfaces, unlike the particles obtained under constant stirring, which have smooth surfaces (Figure 4). Constant stirring gave rise to the formation of prismatic crystals with well-defined facets and salient edges. Along with these individual crystals, crystalline masses are also present. After one hour of the treatment under constant stirring, a greater number of individual prismatic crystals appear, indicating better crystallization with considerably smaller presence of areas of crystalline masses (Figure 5). A closer look at these crystalline masses reveals fractures, which lead to the conclusion that they have a tendency to split and that they can be cleavaged. With a longer treatment, lasting for three hours (Figures 6) the particles become rounded, agglomerated, and shapeless, with diminishing edges. Further, after a treatment prolonged to 15 hours, well-defined crystals can still be observed (Figure 7). Figure 8 displays the morphology of the powder obtained after 100 hours of static solvothermal treatment.

The particle size distributions of the powders (Figures 9 and 10) have a lognormal shape with a high degree of uniformity, showing span values from 1.0 to 1.4 (Table 1). The

results of the particle size analysis (Table 1) support the SEM observations. Generally, when stirring was not applied, smaller particles were obtained, i.e. after 0.5 hours of treatment, the mean particle sizes were 415 nm and 298 nm, with and without stirring, respectively. This means that agitation during the early stages of the solvothermal treatment strongly promotes crystallization, as well as that during prolonged dynamic treatments, dissolution-recrystallization processes of the formed $LiFePO_4$ crystals are involved.

3.2. XRD analysis

The crystal structure of the synthesized powders was confirmed by X-ray powder diffraction. All diffraction patterns revealed a $LiFePO_4$ phase of an olivine-type structure, with no crystalline impurity phases (Figures 11 and 12). The high background noticed after half an hour of the static treatment implies the presence of a significant amount of an amorphous phase. In addition, EDS elemental analysis revealed only the presence of Fe, P, and O (Table 2). Lithium is too light to be detected using EDS. The average molar ratio of iron to phosphorus was close to one, and the largest deviation from one was observed for the powder obtained after half an hour of the static solvothermal treatment. The obtained XRD patterns were compared to the simulated pattern for triphylite with the theoretical isotropic crystal growth and randomly oriented crystallites with the most intense peak (311) at 35.6º (JCPDS #81-1173). Therefore the patterns were normalized to the intensity of the (311) peak. An important feature of the XRD patterns of the synthesized $LiFePO_4$ powders is the peak intensity ratio of I(200)/I(311). Although the XRD patterns were measured for the powdered samples in the same manner, the peak intensity ratio I(200)/I(311) of the samples changed depending on the mode of the solvothermal treatment. The peak intensity of (200) was the strongest in the XRD patterns when continuous stirring was involved, implying the presence of the preferred crystal orientation with a large facet in the bc-plane. Furthermore, the increased peak intensity was observed not only for the (200) reflection but also for all (hk0) reflections (Table 3). Since the growth is perpendicular to a particular set of faces, the slowest growing faces will define the crystal morphology because the fastest growing faces

shrink [25]. This implies that the growth of crystals is preferred along the c-axis. The FACES software enabled us to simulate the external shape (habit) of the crystals by varying the growth rates of the faces of growing crystals, taking into account the surfaces of the lowest energy calculated for LiFePO4 [26]. The simulated external shapes (Figure 13) match well with the actual crystal shapes revealed by the electronic microscopy image. It appears that in our case the most prominent faces of the anisotropic crystal shape are the {100}, {101}, {210}, {201}, and {011} forms, and that the most exposed facet is {100}. On the contrary, when stirring was excluded from the solvothermal treatment, random crystal orientations were obtained with (311) as the most intense reflection and patterns that follow typical intensity ratio for triphylite. The different growth conditions influenced the growth rates of the faces of growing crystals, revealing differences in crystallinity and morphology. The anisotropic crystallite growth, however, can have a significant influence on the preferential orientation of the crystallites, as it was observed during the XRD experiments. Using the X-ray Line Profile Fitting Program (XFIT) with a Fundamental Parameters convolution approach to generating line profiles [27], we calculated the coherent domain sizes of the synthesized powders (Table 4). Greater values of the mean domain sizes for the powders obtained under the dynamic mode confirm that stirring improves crystallization. The variations in the domain sizes follow the same trend as the variations in the mean particle sizes.

3.3. Growth mechanism

The parameters commonly used in hydro(solvo)thermal syntheses to tune the morphology are the reaction temperature and the concentration and chemistry of the surfactant. Dokko et al. [15] have reported that the particle morphology, the crystal orientation, and the electrochemical reactivity of the hydrothermally prepared $LiFePO_4$ particles change depending on the concentration of the Li source and the pH of the precursor. Needle-like particles with a large facet in the bc-plane, or plate-like crystals with a large facet in the ac-plane were obtained by varying pH values. The preferential orientation similar to that obtained in our study was observed when ionic liquids were used as both the solvent and the template to enable the growth of $LiFePO_4$ powders [18]. It has been shown that the

use of ionic liquid with a long alkyl chain (C-18) favors a growth orientation along the [200] direction.

In the present experiments, the syntheses conditions were the same, with no variation in chemical composition, pH, temperature, etc., except for stirring. Accordingly, we tried to explain what differences it could cause. Triton X-100 is a nonionic surfactant that has a hydrophilic polyethylene oxide group and a hydrocarbon lipophilic or hydrophobic group. During strong agitation, water-in-oil emulsion represents the aqueous phase dispersed in the form of droplets surrounded by a monolayer of surfactant and co-surfactant molecules in the continuous hydrocarbon phase. If the stirring is interrupted, the droplets coalesce, and the emulsion separates into two layers: the aqueous phase and the oily phase, with non-spherical dry reverse micelles of Triton X-100 in cyclohexane [28]. It has been recently shown that a dissolution-precipitation mechanism accounts for the hydrothermal synthesis of $LiFePO_4$ platelets when dynamic mode is applied [14]. Yang et al. have suggested that the formation of $LiFePO_4$ is based on the dissolution-recrystallization process along with the phase transformation, when benzyl alcohol is used as a solvent [22]. The initial stages of the solvothermal treatments presented in our study were the same since in both modes, precipitation of an amorphous precursor occured immediately after the mixing of two emulsions at room temperature. During the further stages of the treatment, at a temperature sufficient to promote the precipitation and growth of the desired phase via the Ostwald ripening, which involved the dissolution of fine particles and growth of larger ones, the dissolution-deposition process took place, and the morphology was affected by the kinetics of deposition and the mass transfer to the particle surface. In the dynamic mode, both nucleation and the crystal growth occur in a limited volume of the droplet, surrounded by the surfactant, which, with its polar head, has the ability to bind to some crystal faces, forming inorganic–organic hybrid building blocks [29]. During the process of ripening, the orderly self-assembly hybrid building blocks may coalesce and restructure to produce crystallographically continuous products with the surfactant molecules pealing off. Steric, van der Waals and hydrophilic–hydrophobic interactions involving the pendent chains of the adsorbed surfactants, as well as shape anisotropy, can influence the assembly of the primary particles [29]. In this case, coarsening may operate in a modified Ostwald ripening mechanism in which

orientation, in addition to size, impacts on the survival and consumption of particular grains of a polycrystalline material. Specifically, randomly oriented particles surrounded by coincidentally closely oriented nearest neighbors coarsen and survive, and particles surrounded only by unoriented nearest neighbors are consumed [25]. In the static mode of solvothermal treatment, in which attachment does not occur, the traditional Ostwald type coarsening is predicted to be the predominant mechanism of crystal growth.

3.4. Electrochemical performances

The electrochemical performance of the as-prepared powders obtained after half an hour of both solvothermal treatments were examined by galvanostatic charge–discharge tests. The initial cycles show (Figure 14) that both powders are electrochemically active with discharge capacities of 115 and 107 $mAhg^{-1}$ under the dynamic or static mode, respectively. These values are smaller than the theoretical capacity. It is worth noting that such capacities were obtained without post annealing of the powders or carbon coating. As previously shown, a different mode of preparation resulted in different morphology and crystallinity reflected in different profiles of the charge/discharge curves. The powder obtained under the dynamic mode showed better degree of crystallinity (Table 4), with well-defined crystals preferentially oriented along the bc plane. Its charge/discharge curves show almost flat plateau typical of the two-phased deintercalation/intercalation reaction, with a large voltage gap between curves, indicating the increase of the electrode resistance. The origin of this increased electrode resistance lays in the slow kinetics of lithium ions due to crystal shape. This crystal morphology is not appropriate for Li^+ ion intercalation and deintercalation, because the charge transfer does not occur in the bc crystallographic plane but in the ac-plane [12]. Therefore, the material fails to be fully utilized. The powder obtained under the static mode showed, after a short voltage plateau, sloping curves, which indicate a more homogeneous distribution of lithium ions, which is similar to the cycling behavior of an amorphous $FePO_4$ [30]. Having in mind that the X-ray diffraction analysis of this powder shows the presence of an amorphous phase and that charging was significantly shorter than discharging, which is an indication of lithium deficiency, we assume that the amorphous phase is probably $FePO_4$.

Conclusion

In the present study, we used emulsion-mediated solvothermal route in order to achieve a one-pot synthesis of $LiFePO_4$ particles at a low temperature (180 ºC) without an additional high temperature treatment. The quaternary emulsions of Triton X-100/cyclohexane/*n*-hexanol/water were solvothermally treated for various time periods with and without stirring. It has been found that stirring drastically changes the morphology of $LiFePO_4$ particles, causing the preferential crystal orientation. Apparently, Triton X-100 can selectively adsorb onto certain crystal planes of $LiFePO_4$, thereby decreasing the surface energy, and changing the growth rate of these faces, which causes the growth of anisotropic crystallites with the most exposed {100} facet. Furthermore, greater values of the mean coherent domain sizes for the powders obtained under the dynamic mode confirm that stirring improves crystallization. The powder obtained after only half an hour of the dynamic solvothermal treatment, without additional post annealing or carbon coating, was electrochemically active, showing the discharge capacity of 115 mAh/g. This finding opens the possibility for further examination of emulsion-mediated solvothermal treatments, and the opportunity to tailor the particle morphology by varying the surfactant.

Acknowledgements

The Ministry of Education and Science of the Republic of Serbia provided financial support under grants nos III 45004, III 45015, and III 45014.

References

[1] P. Gibot, M. Casas-Cabanas, L. Laffont, S. Levasseur, P. Carlach, S. Hamelet, J.-M. Tarascon, C. Masquelier, Room-temperature single-phase Li insertion/extraction in nanoscale Li_xFePO_4, Nat. Mater. 7 (2008) 741-747.

[2] M. Gaberšček, R. Dominko, J. Jamnik, Is small particle size more important than carbon coating? An example study on $LiFePO_4$ cathodes, Electrochem. Commun. 9 (2007) 2778 – 2783.

[3] K. Saravanan, M. V. Reddy, P. Balaya, H. Gong, B. V. R. Chowdari, J. J. Vittal, Storage performance of $LiFePO_4$ nanoplates, J. Mater. Chem. 19 (2009) 605–610.

[4] M. Gaberšček, R. Dominko, M. Bele, M. Remškar, D. Hanžel, J. Jamnik, Porous, carbon-decorated $LiFePO_4$ prepared by sol-gel method based on citric acid, Solid State Ionics 176 (2005) 1801-1805.

[5] M. M. Doeff, J. D. Wilcox, R. Kostecki, G. Lau, Optimization of carbon coatings on $LiFePO_4$, J. Power Sources 163 (2006) 180-184.

[6] K. Kim, J. Hwa Jeong, I.-J. Kim, H.-S. Kim, Carbon coatings with olive oil, soybean oil and butter on nano-$LiFePO_4$, J. Power Sources 167 (2007) 524-528.

[7] J.-K. Kim, J.-W. Choi, G. S. Chauhan, J.-H. Ahn, G.-C. Hwang, J.-B. Choi, H-J. Ahn, Enhancement of electrochemical performance of lithium iron phosphate by controlled sol-gel synthesis, Electrochim. Acta 53 (2008) 8258-8264.

[8] M. Konarova, I. Taniguchi, Preparation of carbon coated $LiFePO_4$ by a combination of spray pyrolysis with planetary ball-milling followed by heat treatment and their electrochemical properties, Powder Technol. 191 (2009) 111-116.

[9] C.G. Son, H.M. Yang, G.W. Lee, A.R. Cho, V. Aravindan, H.S. Kim, W.S. Kim, Y.S. Lee, Manipulation of adipic acid application on the electrochemical properties of $LiFePO_4$ at high rate performance, J. Alloys Compd. 509 (2011) 1279–1284.

[10] K. Padhi, K. S. Nanjundswamy, J. B. Goodenough, Phospho-olivines as positive-electrode materials for rechargeable lithium batteries, J. Electrochem. Soc. 144 (1997) 1188-1194.

[11] A. S. Andersson, B. Kalska, L. Häggström, J. O. Thomas, Lithium extraction/insertion in $LiFePO_4$: an X-ray diffraction and Mössbauer spectroscopy study, Solid State Ionics 130 (2000) 41-52.

[12] D. Morgan, A. Van der Ven, G. Ceder, Li conductivity in Li_xMPO_4 (M = Mn, Fe, Co, Ni) olivine materials, Electrochem. Solid-State Lett. 7 (2004) A30-A32.

[13] D. Jugovic, D. Uskokovic, A review of recent developments in the synthesis procedures of lithium iron phosphate powders, J. Power Sources 90 (2009) 538-544.

[14] X. Qin, X. Wang, H. Xiang, J. Xie, J. Li, Y. Zhou, Mechanism for hydrothermal synthesis of $LiFePO_4$ platelets as cathode material for lithium-ion batteries, J. Phys. Chem. C, 114 (2010) 16806–16812.

[15] K. Dokko, Sh. Koizumi, H. Nakano, K. Kanamura, Particle morphology, crystal orientation, and electrochemical reactivity of $LiFePO_4$ synthesized by the hydrothermal method at 443 K, J. Mater. Chem. 17 (2007) 4803–4810.

[16] N. Recham, L. Dupont, M. Courty, K. Djellab, D. Larcher, M. Armand, J.-M. Tarascon, Ionothermal synthesis of tailor-made $LiFePO_4$ powders for Li-ion battery applications, Chem. Mater. 21 (2009) 1096–1107.

[17] Jean-Marie Tarascon, N. Recham, M. Armand, J.-N.l Chotard, P. Barpanda, W. Walker, L. Dupont, Hunting for Better Li-Based Electrode Materials via Low Temperature Inorganic Synthesis, Chem. Mater. 22 (2010) 724–739.

[18] D. Rangappa, K. Sone, T. Kudo, I. Honma, Directed growth of nanoarchitectured $LiFePO_4$ electrode by solvothermal synthesis and their cathode properties, J. Power Sources 195 (2010) 6167–6171.

[19] C. Nan, J. Lu, C. Chen, Q. Peng, Y. Li, Solvothermal synthesis of lithium iron phosphate nanoplates, J. Mater. Chem. 21 (2011) 9994-9996.

[20] F. Teng, S. Santhanagopalan, A. Asthana, X. Geng, S. Mho, R. Shahbazian-Yassar, D. Desheng Meng, Self-assembly of $LiFePO_4$ nanodendrites in a novel system of ethylene glycol–water, J. Cryst. Growth 312 (2010) 3493–3502.

[21] Shiliu Yang, Xufeng Zhou, Jiangang Zhang and Zhaoping Liu, Morphology-controlled solvothermal synthesis of LiFePO4 as a cathode material for lithium-ion batteries, J. Mater. Chem. 20 (2010) 8086–8091.

[22] H. Yang, X.-L. Wu, M.-H. Cao, Y.-G. Guo, Solvothermal synthesis of $LiFePO_4$ hierarchically dumbell-like microstructures by nanoplate self-assembly and their application as a cathode material in lithium-ion batteries, J. Phys. Chem. C, 113 (2009) 3345-3351.

[23] Z. Xua, L. Xua, Q. Lai, Xiaoyang Ji, Microemulsion synthesis of LiFePO4/C and its electrochemical properties as cathode materials for lithium-ion cells, Mater. Chem. Phys. 105 (2007) 80–85.

[24] W. Fan, X. Song, S. Sun, X. Zhao, Microemulsion-mediated hydrothermal synthesis and characterization of zircon-type $LaVO_4$ nanowires, J. Solid State Chem. 180 (2007) 284-290.

[25] R. L. Penn, F. Banfield, Morphology development and crystal growth in nanocrystalline aggregates under hydrothermal conditions: Insights from titania, Geochim. Cosmochim. Acta 63 (1999) 1549 – 1557.

[26] C. A. J. Fisher, M. S. Islam, Surface structures and crystal morphologies of LiFePO4: relevance to electrochemical behaviour, J. Mater. Chem. 18 (2008) 1209-1215.

[27] R. W. Cheary, A. A. Coelho, A fundamental parameters approach of X-ray line-profile fitting, J. Appl. Cryst. 25 (1992) 109-121.

[28] D.-M. Zhu, K.-I. Feng, Z. A. Schelly, Reverse micelles of Triton X-100 in cyclohexane. Effects of temperature, water content, and salinity on the aggregation behavior, J. Phys. Chem. 96 (1992) 2382-2385.

[29] H. Cölfen, S. Mann, Higher-order organization by mesoscale self-assembly and transformation of hybrid nanostructures, Angew. Chem. Int. Ed. 42 (2003) 2350 – 2365.

[30] S. Okada, T. Yamamoto, Y. Okazaki, J. Yamaki, M. Tokunaga, T. Nishida, Cathode properties of amorphous and crystalline $FePO_4$, J. Power Sources 146 (2005) 570-574.

Table 1. The main results of the particle size analysis.

sample		d (0.1) [nm]	d (0.5) [nm]	d (0.9) [nm]	span
dynamic mode	0.5 h	296	415	833	1.33
	1 h	299	421	879	1.38
	3 h	234	330	565	1.00
	15 h	351	505	1000	1.46
static mode	0.5 h	215	298	525	1.04
	15 h	254	353	695	1.25
	100 h	250	351	627	1.07

Table 2. The results of EDS elemental analysis.

sample		Fe (at.%)	P (at.%)	O (at.%)
dynamic mode	0.5 h	12.65	12.42	74.93
	1 h	11.18	11.96	76.86
	3 h	12.64	12.87	74.48
	15 h	10.51	11.76	77.73
static mode	0.5 h	14.02	12.93	73.05
	15 h	12.80	12.44	74.76
	100 h	15.80	13.32	70.88

Table 3. The peak intensity ratio I(hk0)/I(311) of the samples obtained under dynamic solvothermal treatment.

(hkl) / sample	(200)	(210)	(410)	(610)
0.5 h	2.6	0.5	0.9	1.06
1 h	4.2	0.6	1.0	1.0
3 h	1.8	0.5	0.6	0.6
15 h	2.3	0.6	0.8	0.9
JCPDS 81-1173	0.4	0.3	0.2	0.2

Table 4. Mean domain sizes.

	sample	mean domain size [nm]
dynamic mode	0.5 h	118
	1 h	192
	3 h	185
	15 h	208
static mode	0.5 h	83
	15 h	196
	100 h	346

Figure captions

Fig. 1. Crystal structure of the olivine-type $LiFePO_4$ viewed along the b axis (direction of lithium ion diffusion).

Fig. 2. Scheme of the experimental apparatus: 1- magnetic stirrer hotplate, 2 – thermo-isolating layer, 3 – temperature probe, 4 – glass beaker, 5 – silicon oil, 6 - Teflon-lined stainless steel autoclave, 7- reaction emulsion, 8 – magnetic stir bar.

Fig. 3. FESEM image of the powder obtained after half an hour of static solvothermal treatment.

Fig. 4. FESEM image of the powder obtained after half an hour of dynamic solvothermal treatment.

Fig. 5. FESEM image of the powder obtained after 1 h of dynamic solvothermal treatment.

Fig. 6. FESEM image of the powder obtained after 3 h of dynamic solvothermal treatment.

Fig. 7. FESEM image of the powder obtained after 15 h of dynamic solvothermal treatment.

Fig. 8. FESEM image of the powder obtained after 100 h of static solvothermal treatment.

Fig. 9. Particle size distributions for $LiFePO_4$ powders obtained under static solvothermal treatment.

Fig. 10. Particle size distributions for $LiFePO_4$ powders obtained under dynamic solvothermal treatment.

Fig. 11. XRD patterns of $LiFePO_4$ powders synthesized under static solvothermal treatment for various time. At the bottom is simulated XRPD pattern for triphylite with isotropic crystallites and random orientation in accordance with JCPDS 81-1173.

Fig. 12. XRD patterns of $LiFePO_4$ powders synthesized under dynamic solvothermal treatment for various time. At the bottom is simulated XRPD pattern for triphylite with isotropic crystallites and random orientation in accordance with JCPDS 81-1173.

Fig. 13. Some simulated morphologies of the observed crystal morphologies obtained by using software FACES.

Fig. 14. The initial charge/discharge curves of the powders obtained solvothermally under dynamic and static mode at C/10 current rate.

Figure 1.

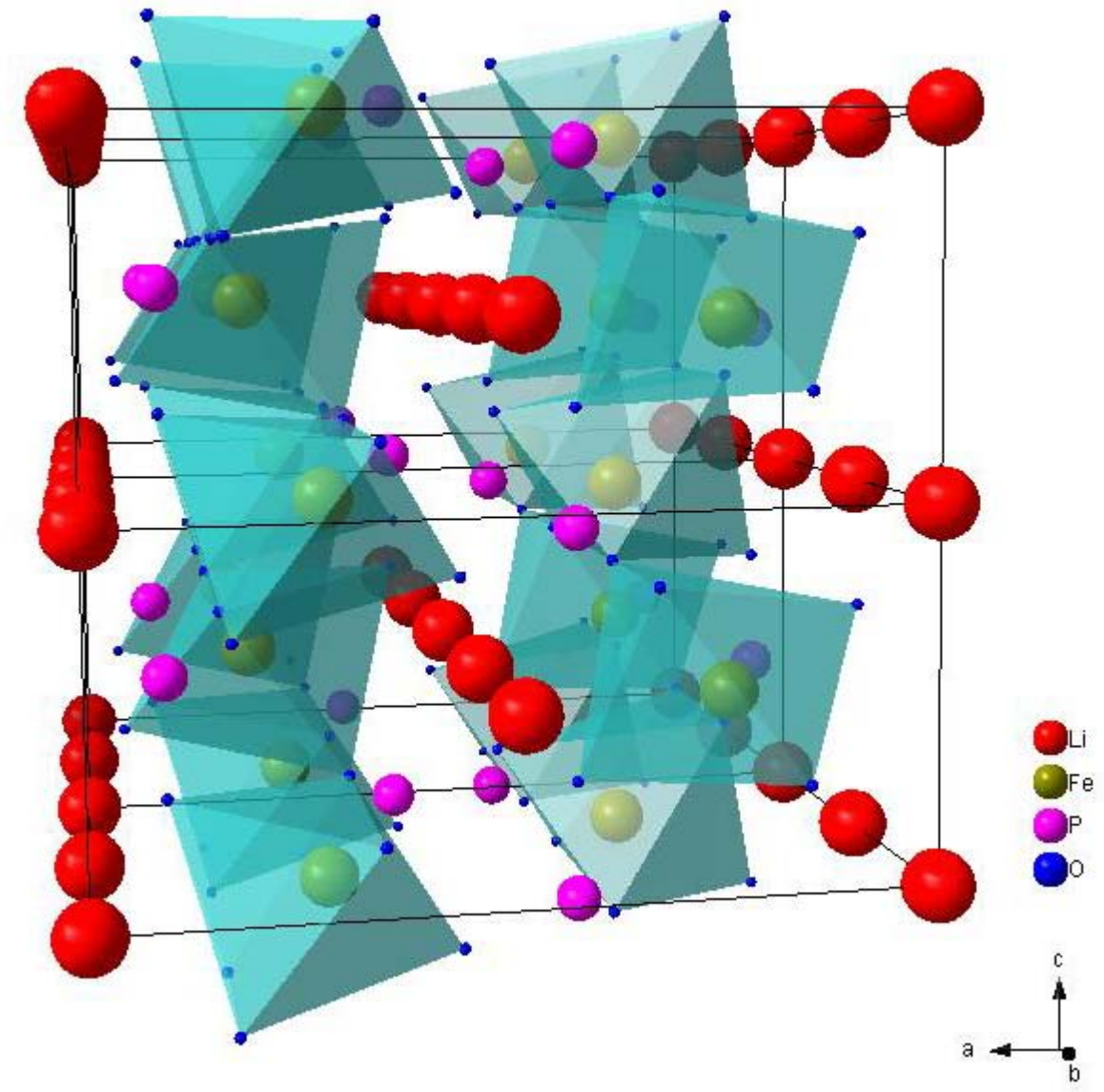

Figure 2.

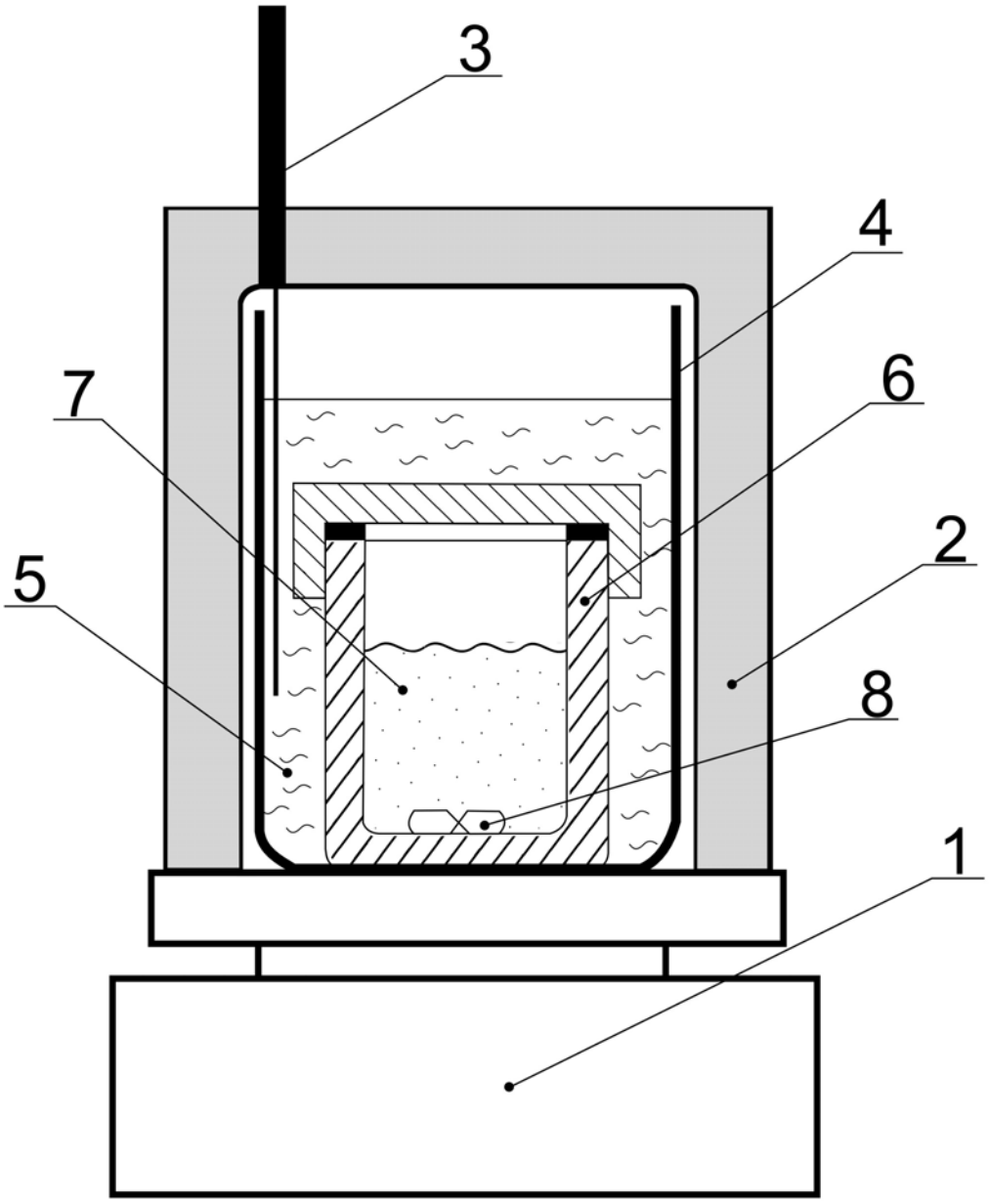

Figure 3

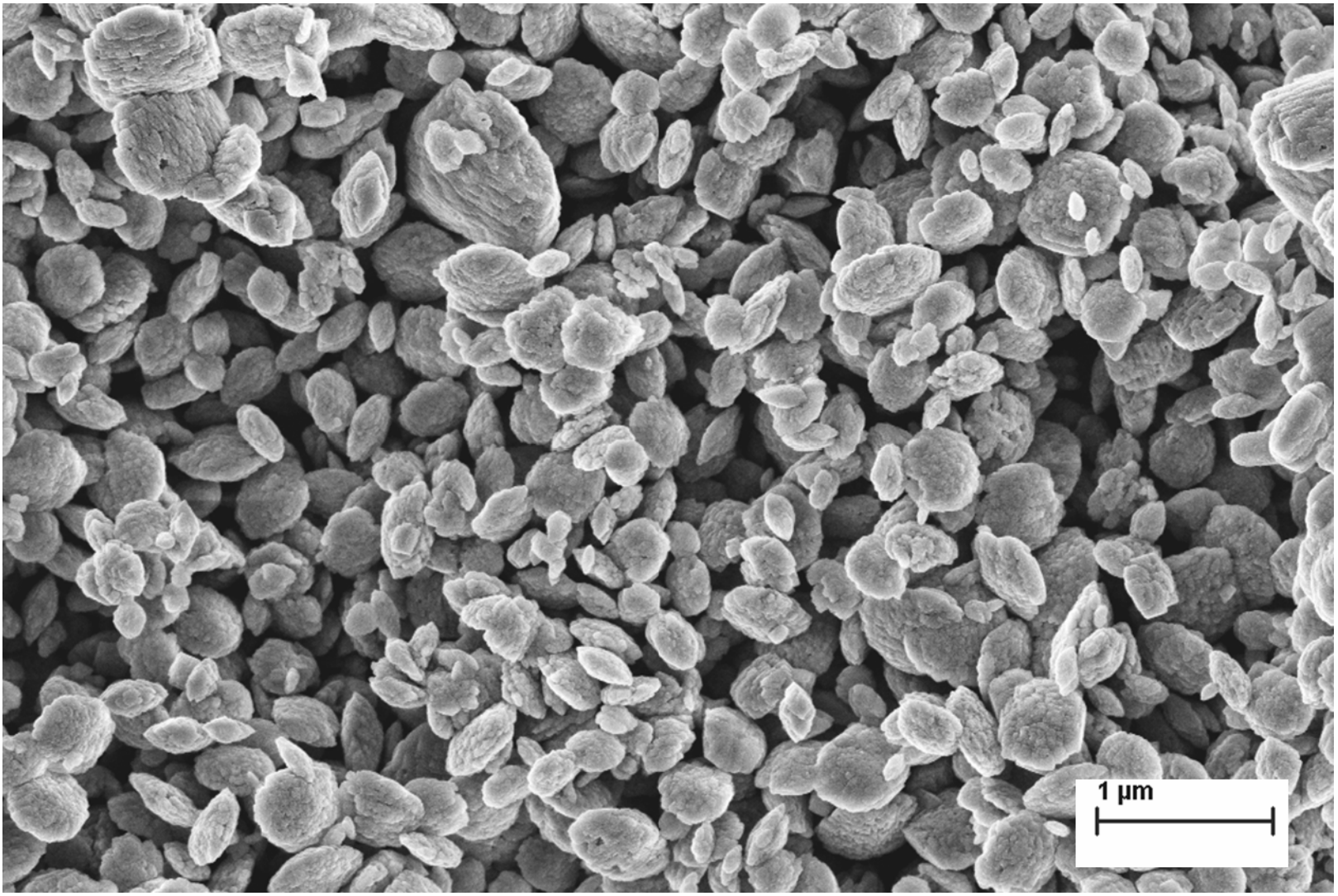

Figure 4

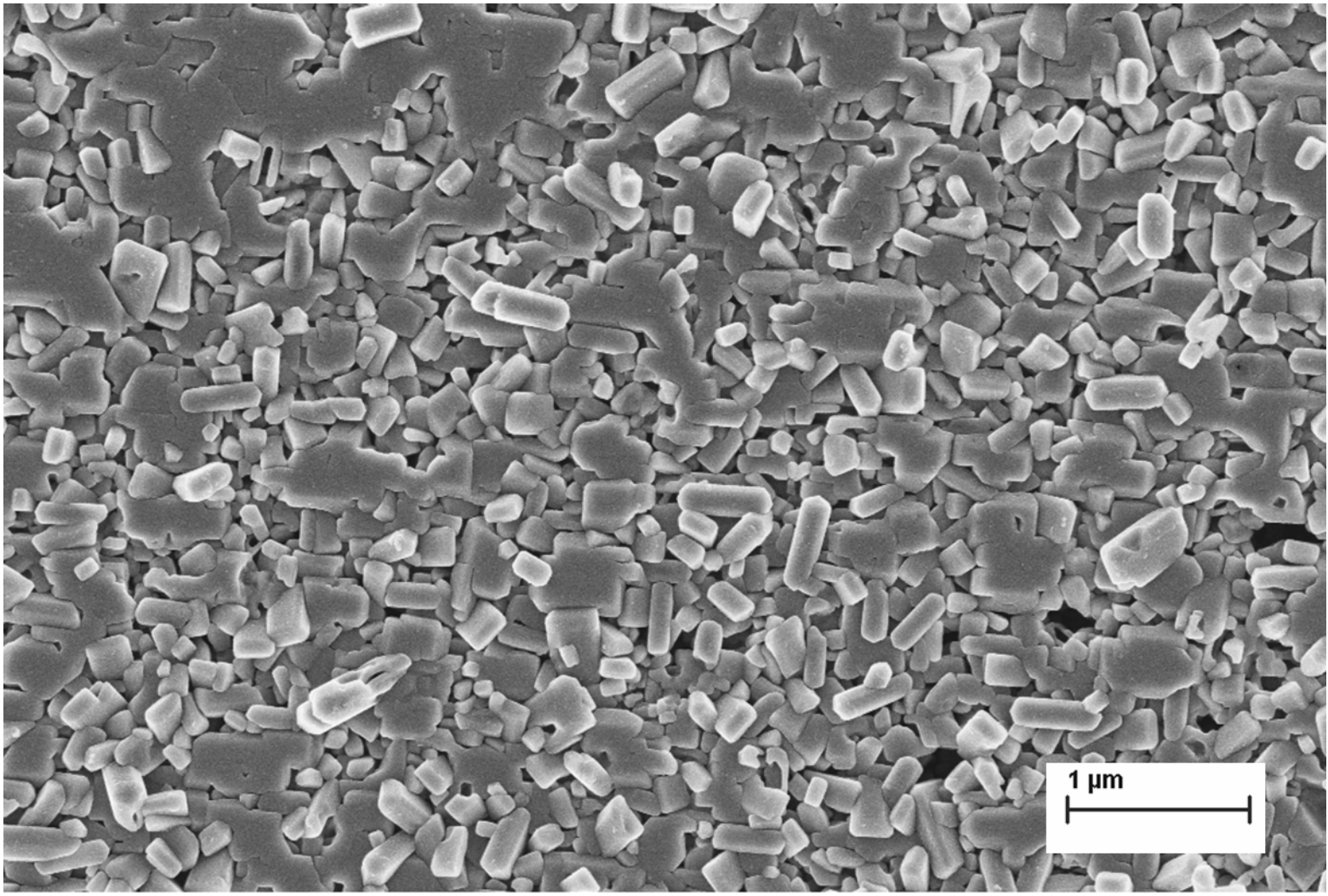

Figure 5

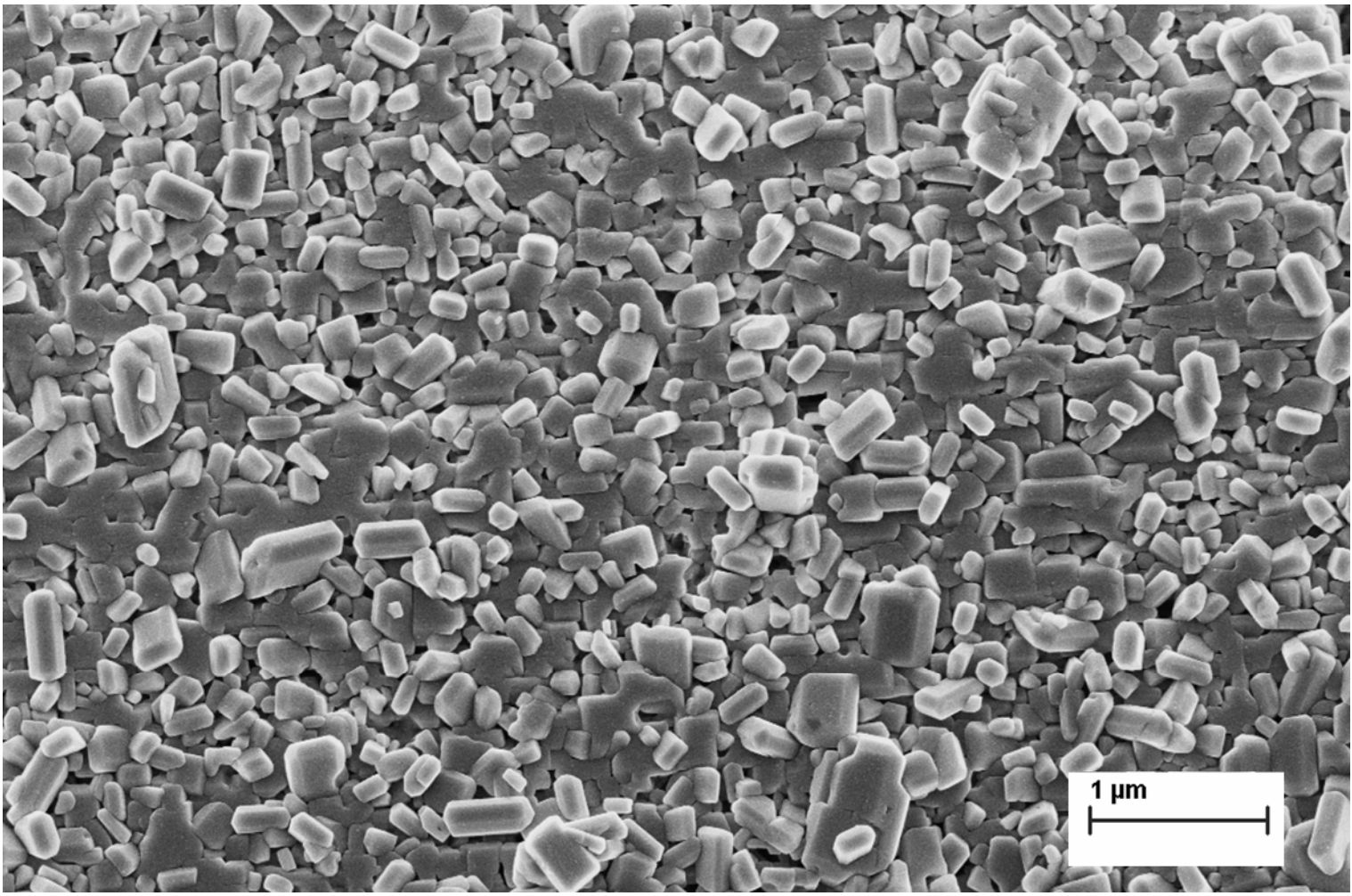

Figure 6

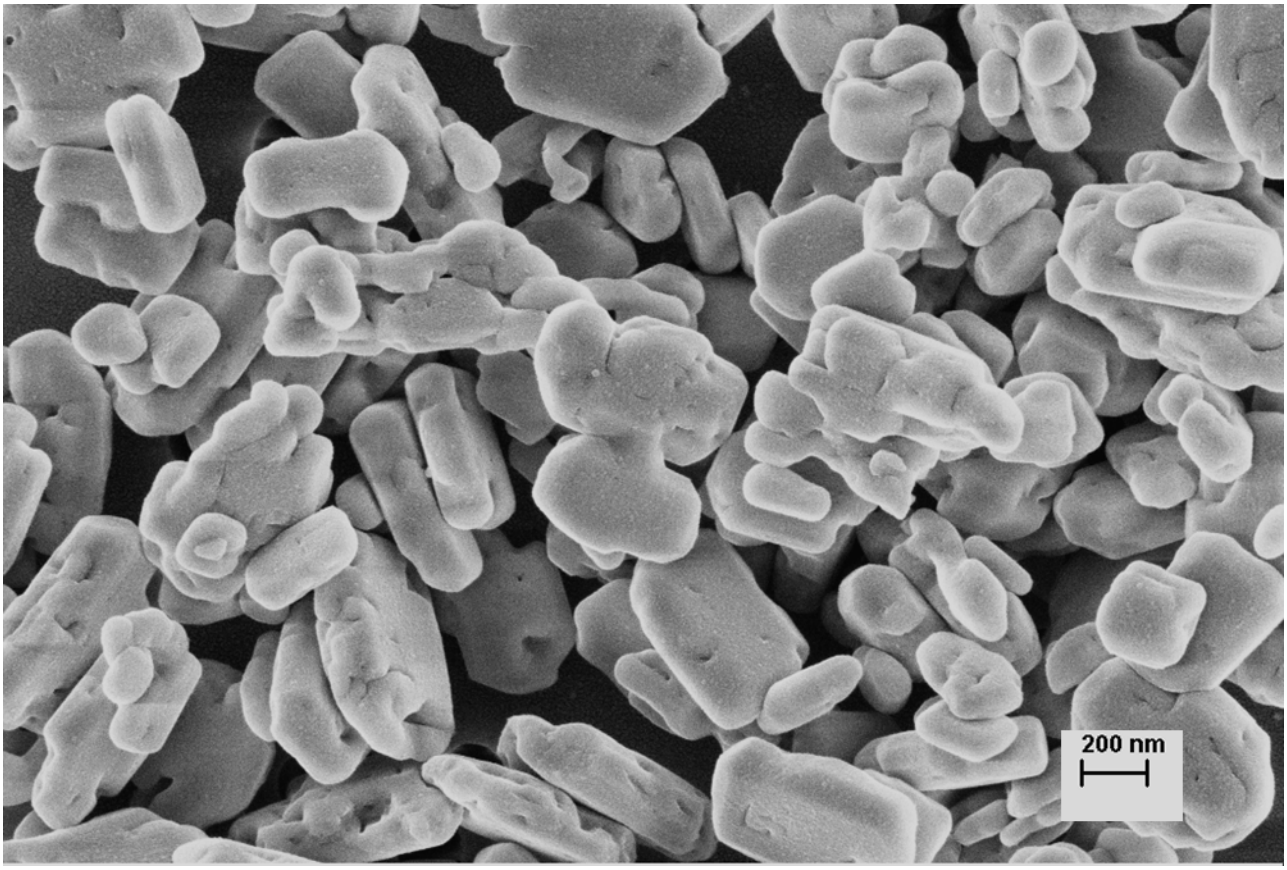

Figure 7

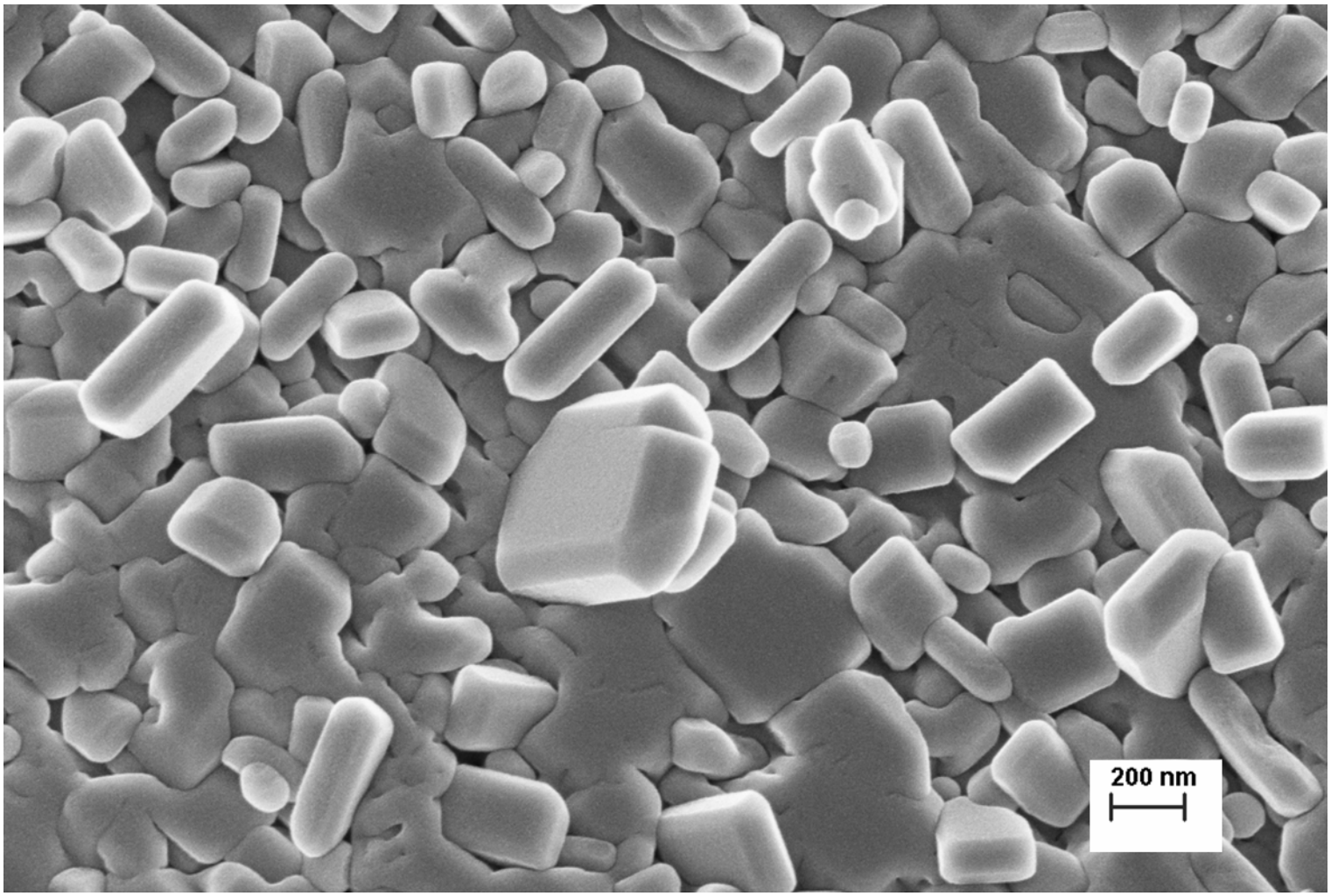

Figure 8

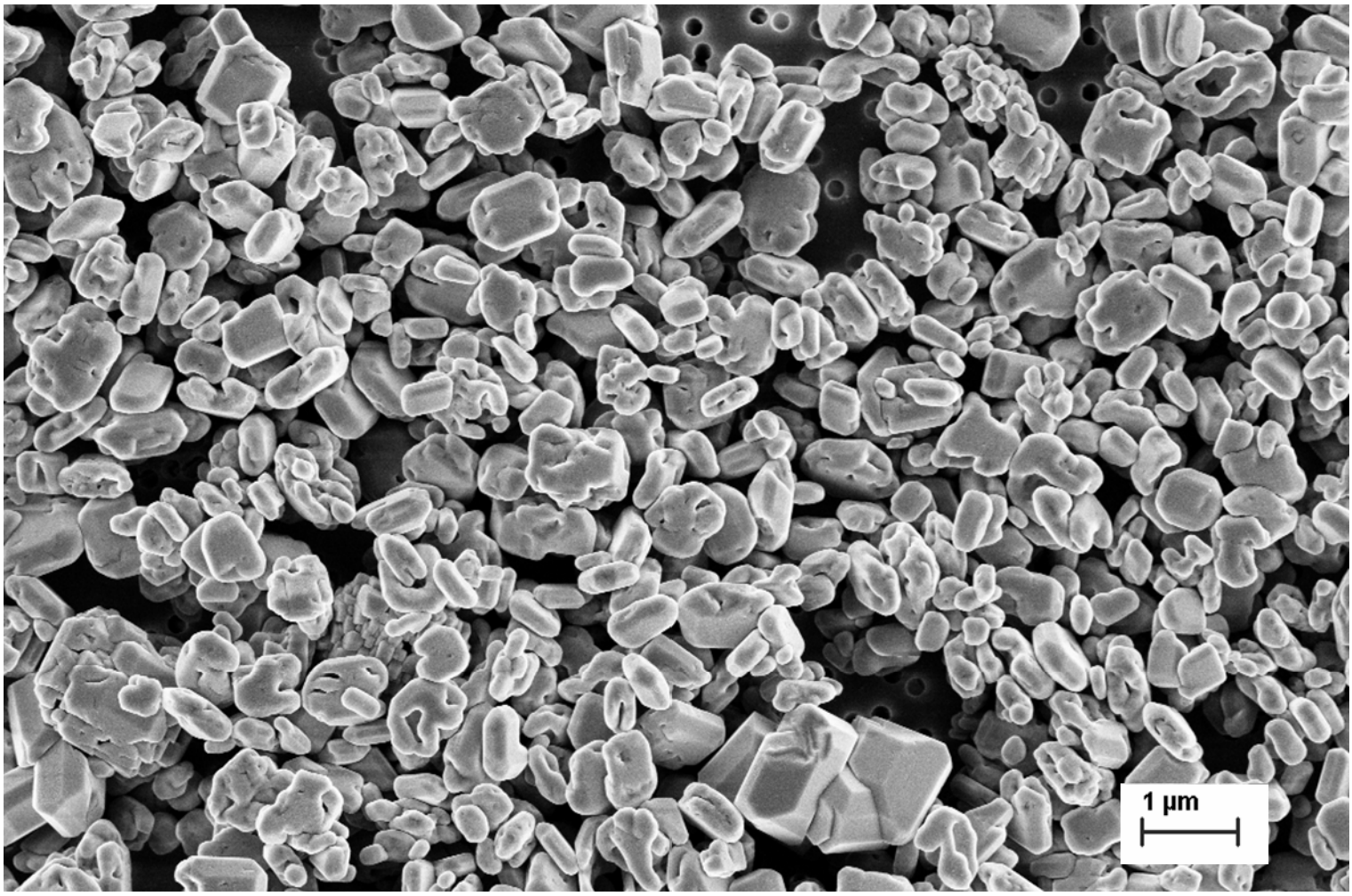

Figure 9

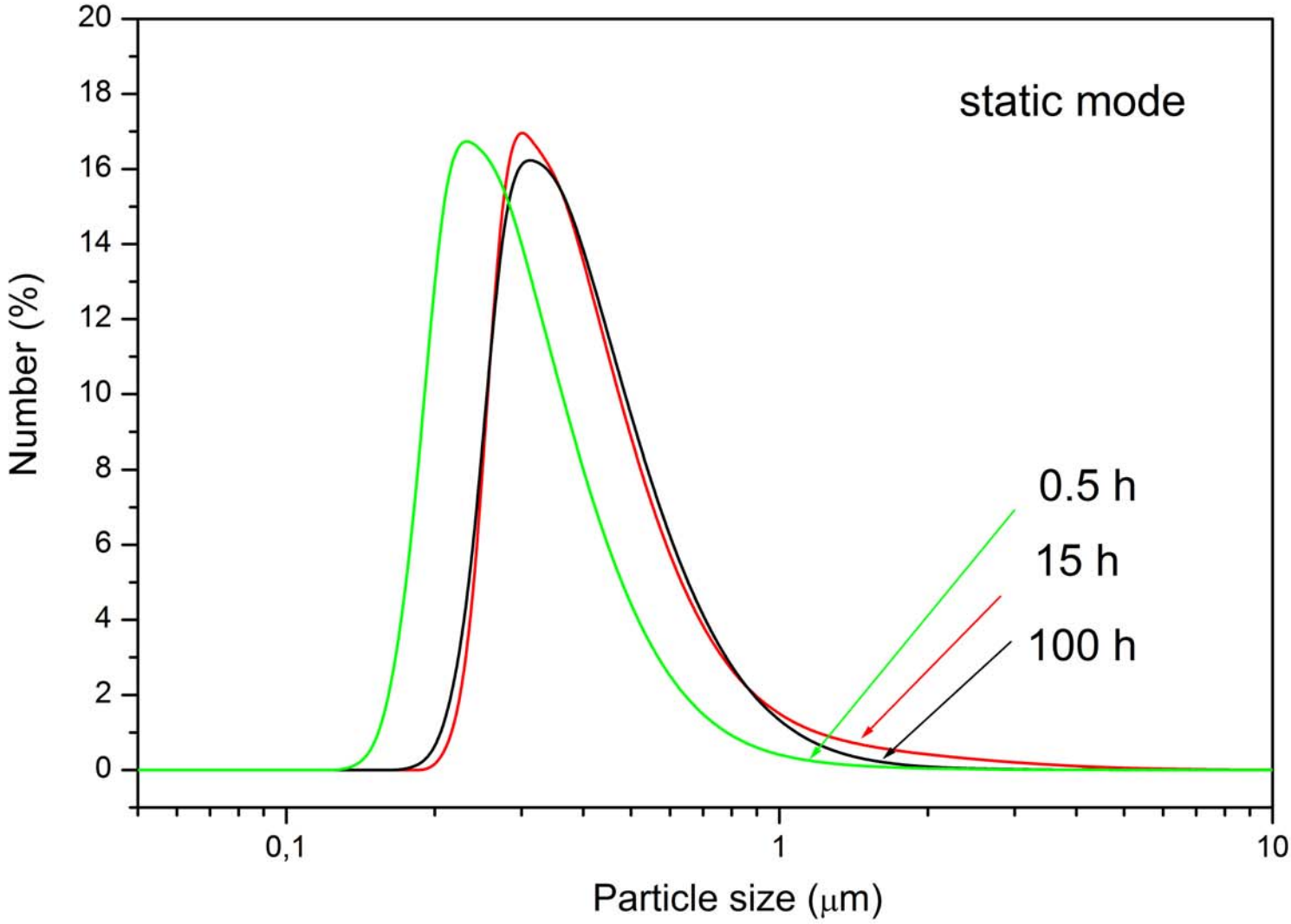
static mode
0.5 h
15 h
100 h
Number (%)
Particle size (μm)
0
2
4
6
8
10
12
14
16
18
20
0,1
1
10

Figure 10

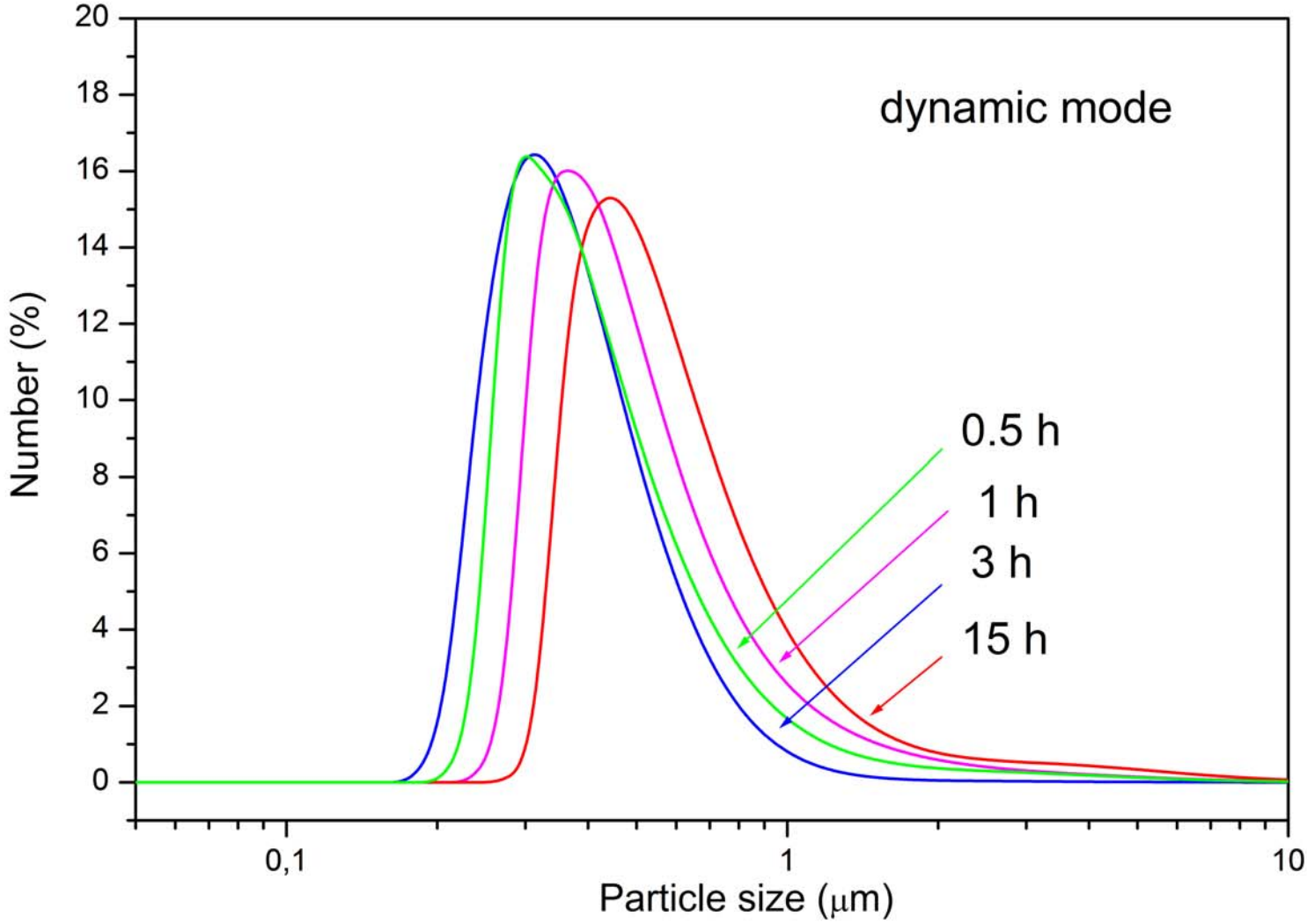
dynamic mode
0.5 h
1 h
3 h
15 h
Number (%)
Particle size (μm)
0
2
4
6
8
10
12
14
16
18
20
0,1
1
10

Figure 11

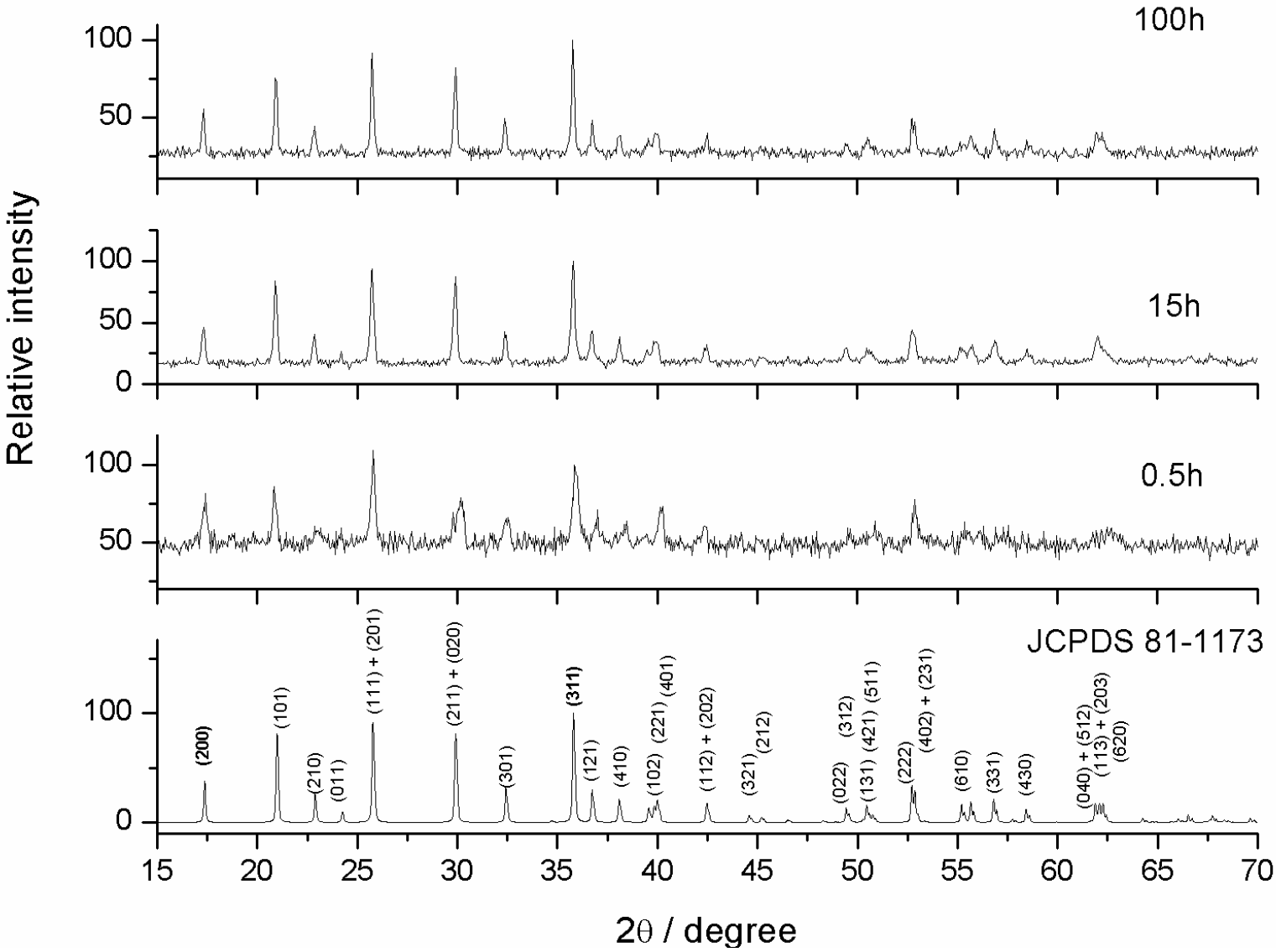
100h
15h
0.5h
JCPDS 81-1173
Relative intensity
2θ / degree
(200)
(101)
(210)
(011)
(111) + (201)
(211) + (020)
(301)
(311)
(121)
(410)
(102)
(221)
(401)
(112) + (202)
(321)
(212)
(022)
(312)
(131)
(421)
(511)
(222)
(402) + (231)
(610)
(331)
(430)
(040) + (512)
(113) + (203)
(620)

Figure 12

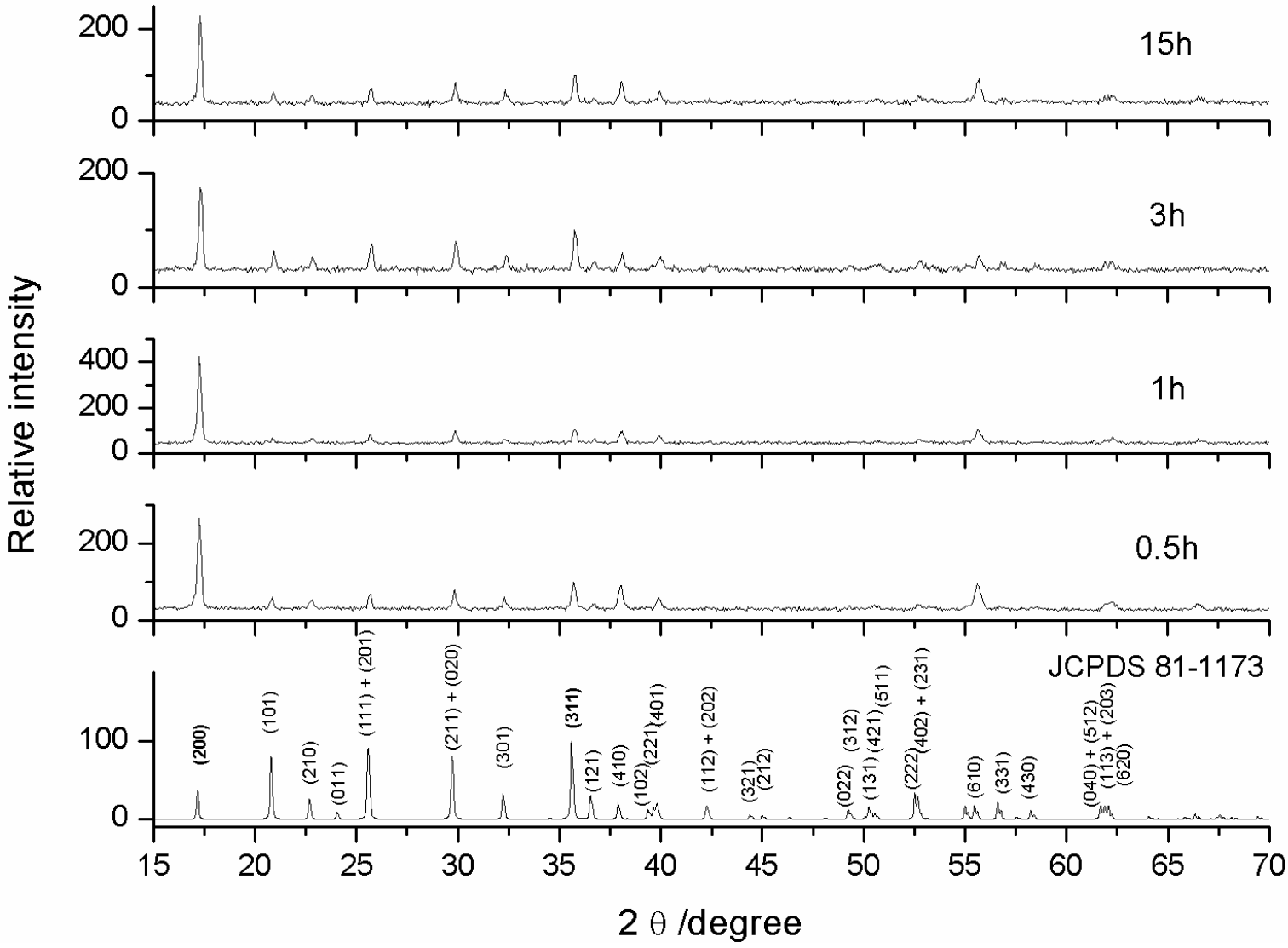
15h
3h
1h
0.5h
JCPDS 81-1173
Relative intensity
2 θ /degree
(200)
(101)
(210)
(011)
(111) + (201)
(211) + (020)
(301)
(311)
(121)
(410)
(102)
(221)
(401)
(112) + (202)
(321)
(212)
(022)
(312)
(131)
(421)
(511)
(222)
(402) + (231)
(610)
(331)
(430)
(040) + (512)
(113) + (203)
(620)

Figure 13

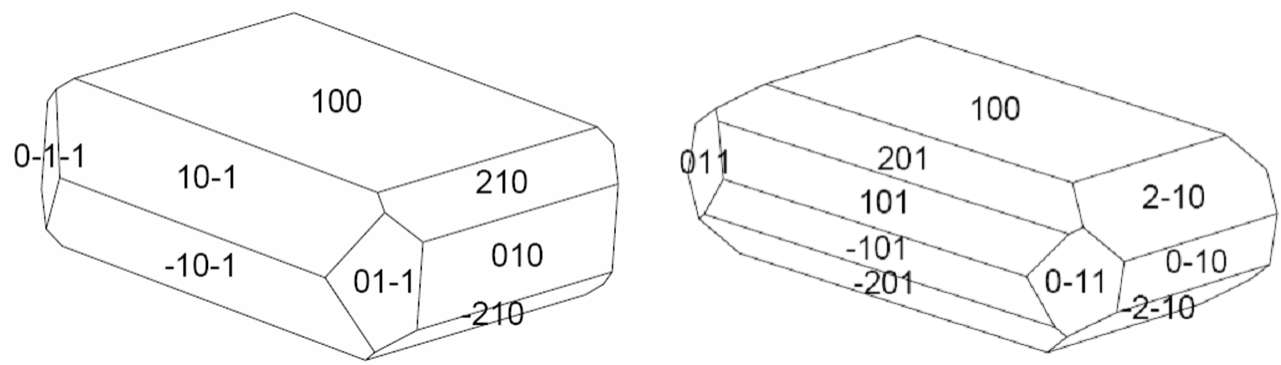
100
0-1-1
10-1
210
-10-1
01-1
010
-210
100
011
201
101
2-10
-101
0-10
-201
0-11
-2-10

Figure 14

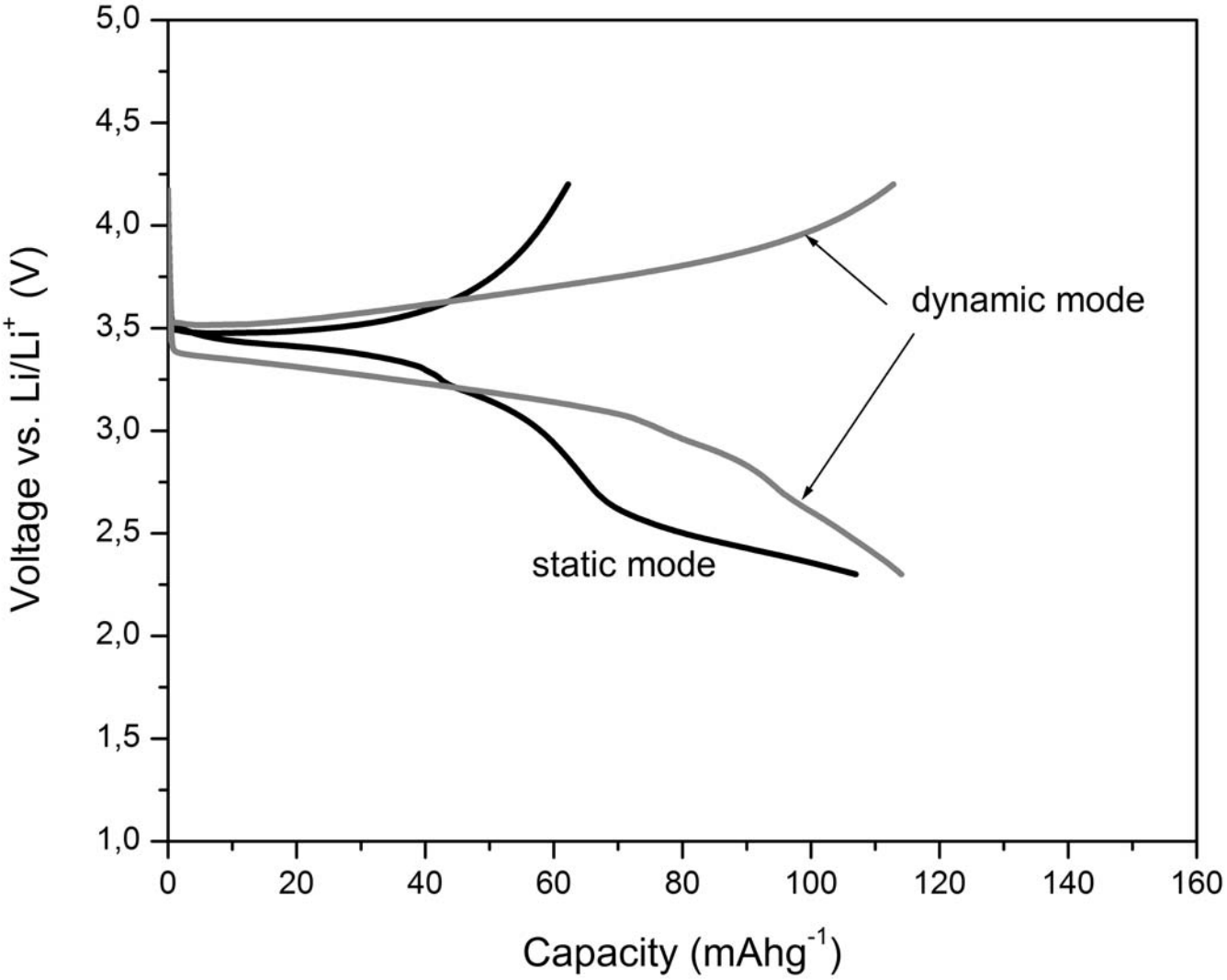
5,0
4,5
4,0
3,5
3,0
2,5
2,0
1,5
1,0
0
20
40
60
80
100
120
140
160
Voltage vs. Li/Li+ (V)
Capacity (mAhg-1)
dynamic mode
static mode